DOI : https://doi.org/10.56452/96

ISSN: 0974-5823 Vol. 7 (Special Issue 5, June 2022)

International Journal of Mechanical Engineering

MECHANICAL PROPERTIES OF LANTHANUM ZIRCONATE AND LANTHANUM PHOSPHATE SPRAYED INCONEL BASED THERMAL BARRIER COATINGS

Bhalachandra Patil[a], R Keshavamurthy[b]

[a]PG Sudent Department of Mechanical Engineering, Dayananda Sagar College Of Engineering, Shavige Malleshwara Hills, 91st Main Road, 1st Stage, Kumaraswamy Layout, Bangalore, 570078, India

[b]Professor Department of Mechanical Engineering, Dayananda Sagar College Of Engineering, Shavige Malleshwara Hills, 91st Main Road, 1st Stage, Kumaraswamy Layout, Bangalore, 570078, India

Abstract. Thermal Barrier Coatings are extremely cutting-edge material solutions that are frequently applied to metallic surfaces that function at high temperatures, such as parts of aero-engines or gas turbines. These coatings are used on a frequent basis on these types of surfaces because they are effective at preventing heat transfer. In order to improve turbine efficiency and extend the useful life of metallic components, aero-turbine engines frequently make use of composite materials consisting of multiple layers of ceramic and metal. Coatings of varying types are applied to a wide variety of technical materials in order to protect them from elements such as corrosion, wear, and erosion. The thermal barrier coatings (TBCs) are the most important of these because they insulate against heat and protect the material from high temperatures. This research looks at the thermal barrier coatings that are made from lanthanum zirconate and lanthanum phosphate, and discusses their respective mechanical properties. The ceramic-based coatings are tested for their hardness as well as their young's modulus, and the results are analysed and compared with an uncoated substrate.

Keywords – Thermal barrier coatings, plasma spray coatings, ceramic coatings.

1. Introduction

Thermal barrier coatings, also known as TBCs, are required for insulating components of engines that operate at high temperatures. Some examples of these components include aero engine parts and gas turbines. Combustion chambers, nozzle guiding vanes, turbine blades, and ductwork are a few examples of such components. The development of TBCs has made it practicable to run gas turbines at higher temperatures. Because of their exceptionally low thermal conductivity, TBCs are particularly resistant to the flow of heat; as a result, when they are subjected to it, the coating will dramatically increase in temperature. The most common type of TBC material is called yttria-stabilized zirconia (YSZ), and it has the ability to withstand thermal shock and fatigue up to 1150 degrees Celsius. Electron beam physical vapour deposition, also known as EBPVD, and plasma spraying are two methods that are frequently utilised for the deposition of YSZ. It is also possible to spray it with high-velocity oxygen fuel (HVOF), which takes advantage of the wear-resistant properties of the material and can be used for applications such as preventing wear on the blade tip. [1-3]

The two methods that are utilised the most frequently in the production of YSZ are plasma spraying and

DOI : https://doi.org/10.56452/96

electron beam physical vapour deposition (EBPVD) with an electron beam. In order to take advantage of the wear-resistant properties of the material, HVOF can be sprayed on it and applied in such a way as to prevent wear on the blade tip.

The primary purpose of TBCs is to act as thermal barriers; however, due to the extremely hostile thermo-mechanical environment in which they operate, they are required to adhere to a number of stringent performance standards in addition to serving their primary purpose. In order for the coatings to be able to withstand the thermal expansion stresses brought on by heating and cooling, whether as a result of regular operation or a "flame-out," they need to be able to withstand extremely high strains without breaking. When producing the coating with electron-beam evaporation or plasma spraying, for example, porosity is typically added to the microstructure to accomplish this strain compliance. [4-8]

Ceramic material known as lanthanum zirconate, also known as $La_2Zr_2O_7$ or LZ, has a pyrochlore structure that is distinctive to this material. The structure of pyrochlore is typically represented by the chemical formula $A_2B_2O_7$. In the formula for $A_2B_2O_7$, the element A is most frequently a rare earth or an element that only possesses a single pair of electrons, whereas the element B can either be a transition metal or a post-transition metal and has a variable oxidation state. For TBC applications, LZ offers a number of advantages over 8YSZ, including the following: (1) there is no phase transition from room temperature to melting temperature; (2) strong sintering resistance; (3) low thermal conductivity (1.5-1.8 W/m/K for completely dense material at 1000 °C); and (4) LZ has a lower oxygen ion diffusivity, which prevents oxidation of the bond coat and the substrate. The fact that LZ has a low value of CTE is the most significant drawback of using this material. This value does not correspond to the high CTE values of the substrate or the bond coat. [7-10]

Both lanthanum phosphate and lanthanum zirconate have high melting point and does not react with molten minerals. In high-temperature applications, coatings made of lanthanum phosphate and lanthanum zirconate are frequently used to protect vital components from the corrosion that can be caused by reactive molten metals. In the current investigation, it is proposed that lanthanum zirconate and lanthanum phosphate have been sprayed using an air plasma spray method, and then the mechanical properties of the resulting materials are characterised.

2. Experimentation

2.1 Material used and Deposition of Coating

As the deposition for coating feedstock material, commercial-grade powdered lanthanum zirconate and lanthanum phosphate were utilised. The substrate, which consisted of plates made of an alloy called Inconel-625 and had dimensions of 100 millimetres on each side, was sandblasted and thoroughly cleaned with acetone in order to improve the bonding property across the interface of the coating. After that, a bond coat made of NiCr with a thickness of 50 m was applied to the substrate. The thickness of the top layers of lanthanum phosphate and lanthanum zirconate that were deposited using a Suzler-Metco 3MB Plasma torch was 100 metres. Throughout the entire process of deposition, a voltage of 60 Volts was maintained despite the utilisation of Argon and Hydrogen as carrier gases. The plasma spray coating was carried out in Spraymet Surface Technologies Pvt Ltd, Peenya, Bengaluru using plasma arc gun and the parameters involved in the process is shown in Table 1.

DOI : https://doi.org/10.56452/96

Table 1: Process parameters for plasma spray coating

Parameters	Value	Pressure	Flow rate
Type of Primary plasma gases	Ar/ 50 Sl/ min	100-120 psi	80-90 SCFH
Type of Secondary plasma gases	H_2/ 14 Sl/ min	50 psi	15-18 SCFH
Diameter of anode nozzle	6mm		
Current arc	500A		
Voltage arc	66-70V		
Stand – off distance	100mm		
Powder speed	40-45 /min		

The most adaptable process, thermal spray coating appears to be a well-liked, practical, and affordable surface engineering method. As a result, thick coatings with a range of surface qualities will emerge, which will be beneficial for many technical components working under difficult circumstances.

In this method, a layer is created by projecting well-melted and semi-molten, softened materials onto a component's surface. Upon impact, these materials flatten out fast and solidify. The deposition of platelets known as splats, which are produced as a result of repetitive particle impacting, mechanically interlocks with the target surface, resulting in coatings that range in thickness from 50 m to a few millimeters. This method is gaining popularity for creating goods that compete with similar products already on the market and satisfy all the requirements of diverse surface phenomena.

The common practice of using rod wire and powder to feed coating ingredients. Real materials are used, ranging from ceramics with high melting temperatures to low melting materials like plastics. The coating material is heated to a molten or semi-molten state via plasma spraying, which makes use of the thermal plasma's high temperature and high velocity. Spraying any powder into the plasma plume causes it to melt and move faster in the direction of the substrate. In order to strike the surface of the chosen substrate, the molten powder particles are accelerated to high speeds (100-200 m/s). The molten particles form a very sticky covering when they strike the substrate and attach to one another. For the purposes including corrosion resistance, thermal barrier coatings, erosion, abrasion resistance, and unique coatings like superconductive coatings, this process is typically employed to produce a variety of protective coatings on metals and alloys.

2.2 Testing and Characterization

In the present work, Inconel 625 is chosen as a base material. It is a super alloy and is in sheet form. High-strength nickel-chromium alloy Inconel is very easy to work with, even when putting this methodology relies on top-down methods that shrink the size of the bigger pieces and are comparable to particle self-assembly. The stainless steel ball milling process was applied to the dry powder samples that were put in the vessel of a small ball milling apparatus. Following the vessel's initial rotation, the steel balls in the tank ground the powder samples. The next set of settings were applied during ball milling: Ten steel balls weighing 40.4g apiece, a small ball mill rotating at 300rpm, and a ball to powder ratio of 10:1 were used to grind the composite powders.

The vessel was properly filled with the powder sample(s) and sealed. The rotating activity of the vessel causes the steel balls within to collide with one another and the container. Following that, SEM studies were conducted at BMS College of Engineering (VEGA3 TESCAN), Bengaluru, India. To investigate the morphology, surface topography feedstock powders and coatings. Nano-indentation was performed at CMTI in Bengaluru. ASTM E 2109 was used to determine the elastic modulus and hardness of polished coated samples (method A). The optical microstructure of composites was studied at the Advanced Metallurgical Laboratory in Peenya, Bengaluru. All the inconel samples were examined under an optical microscope.

DOI : https://doi.org/10.56452/96

Samples were metallographically polished before being characterized using various grades of emery sheets on a lap grinding machine. To remove dirt and contaminants from the specimen's testing surface, the samples were cleaned and polished in cloth with an Acetone (99.9% purity) solution. Then, at BMS College of Engineering (X'Pert system), Bengaluru, XRD is performed on two powders. The crystalline phases present in the material are identified using XRD analysis, which reveals chemical composition information. Lanthanum zirconate and lanthanum phosphate were used to coat the inconel plate.

3. Results and Discussion

3.1 Feedstock Powder Morphology

The feedstocks, Lanthanum Zirconate and Lanthanum phosphate powder, were examined using SEM and energy-dispersive X-ray spectroscopy to determine their shape and phase composition (EDAX). The lanthanum zirconate powder's typical particle size in the SEM picture of Figure.1 (a) is between 20 and 50 µm, and it has a spherical form. and Lanthanum Phosphate Powder are both significantly cuboidal in shape. EDAX patterns, as shown in Figure. 2 and 3, respectively, demonstrate the existence of essential elements in the feedstock powders for lanthanum zirconate and lanthanum phosphate.

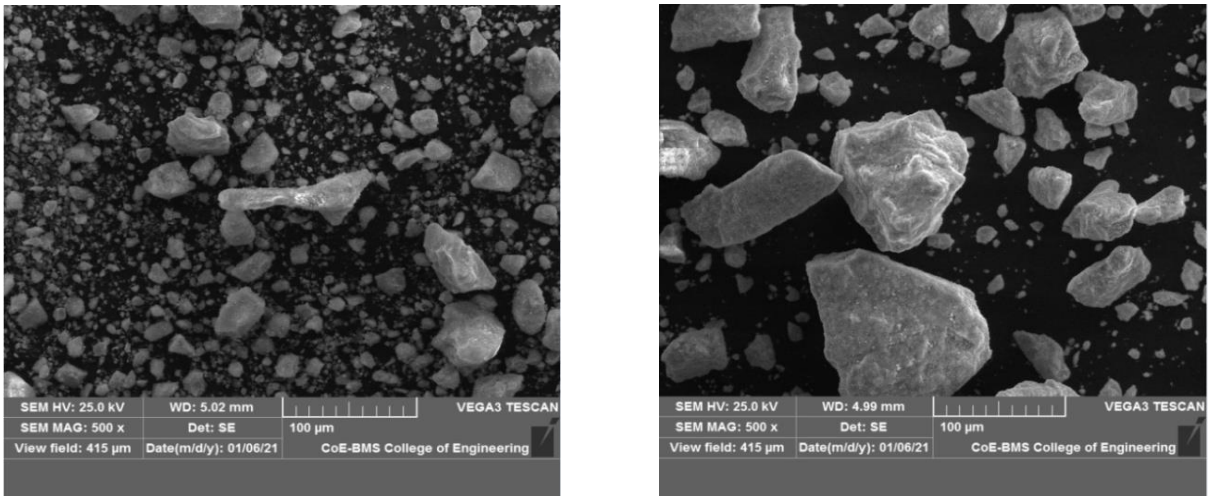

(a) (b)

Figure 1. SEM Images : (a) Lanthanum Zirconate powder; (b) Lanthanum Phosphate powder

To determine the thickness and compositions, the coatings cross section was examined. In MPC, the covering was around 25 mm thick. Although the two samples had roughly the same thickness of 22 mm, micro-structural examination revealed that the coatings really had two separate layers. Figure 4. displays the comprehensive study of the sample coating's cross section. EDS examination of several coating locations is also shown in Figure 2 and 3. The EDS examination revealed a larger proportion of Mg and P with a low percentage of La content in the bottom layer, which was characterized as a composite layer of struvite and newberyite. Similar to this, an EDS examination of the uppermost layer (10 to 12 µm) revealed a high proportion of La and a comparatively low percentage of Mg. The results of the SEM and EDS analyses supported the hypothesis that the lanthanum phosphate coating was composed of two layers, the bottom layer being a rich magnesium phosphate layer composed of struvite and newberyite and the top layer being a rich layer of lattice oxygen (LaPO4) and less magnesium phosphate.[8]

DOI : https://doi.org/10.56452/96

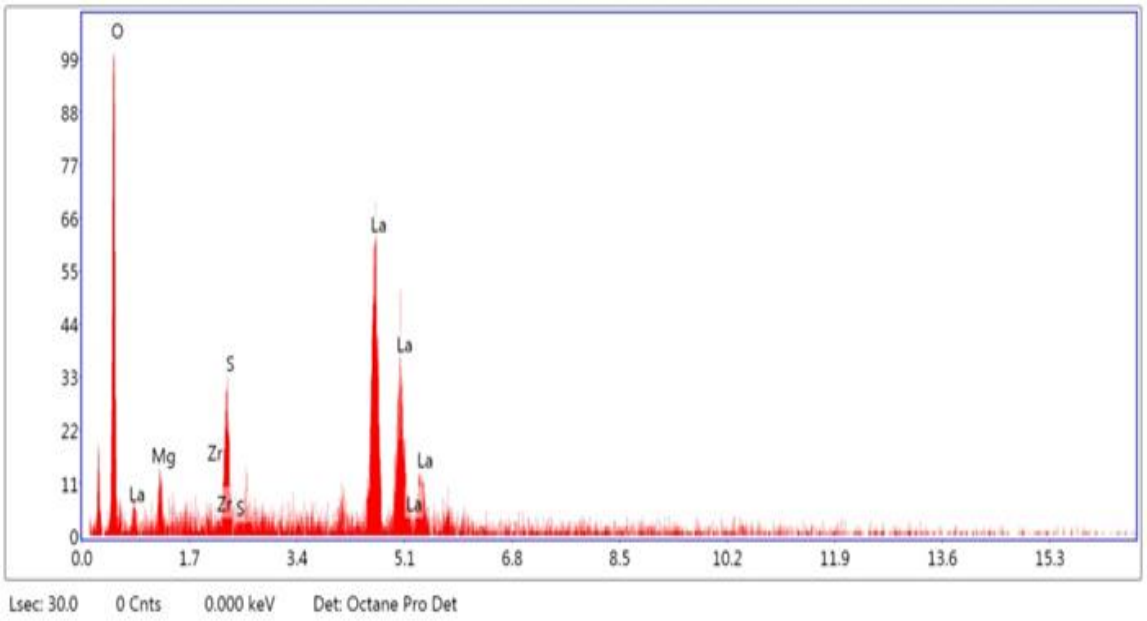

Figure 2. EDAX pattern of Lanthanum Zirconate particles

Figure.2 shows EDAX report of lanthanum zirconate particles which verifies the presence of key components in utilized feedstock powder.

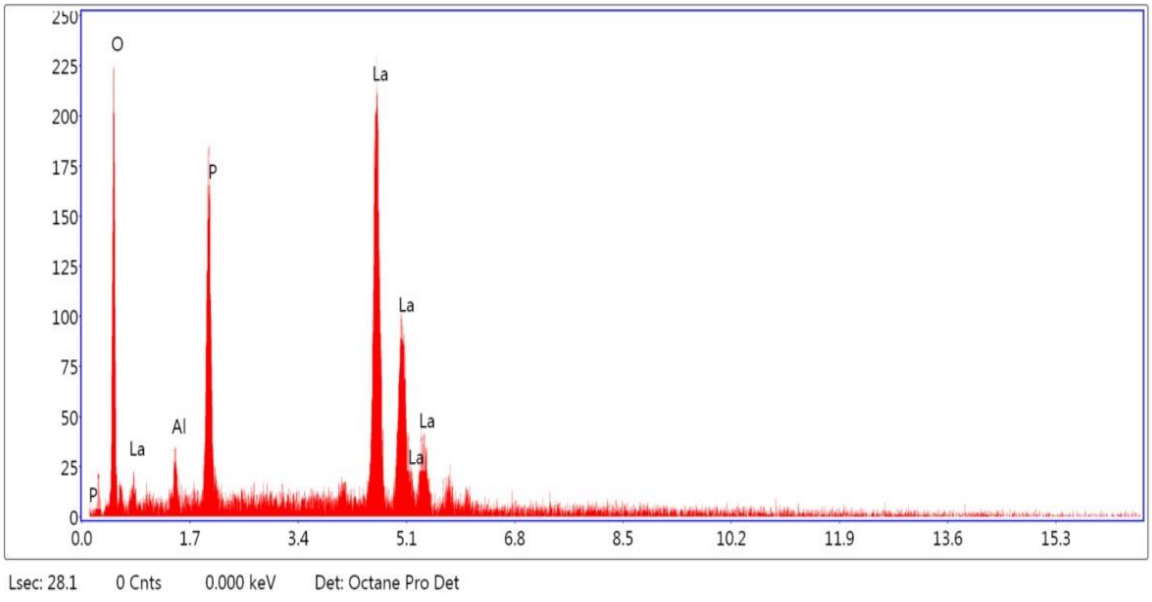

Figure 3. EDAX pattern of Lanthanum Phosphate paricles

Figure.3 shows EDAX report of lanthanum phosphate powder which verifies the presence of key components in utilized feedstock powder.

In Figure 3, which depicts the $LaPO_4$ particle distributions, the particles are distributed evenly throughout the material. Further from Figure.3 data provided together with a semi-quantitative elemental composition of atomic percent and weight percent on the shattered areas. With contributions of 57 weight %, 11.62 weight %, and 31.18 weight %, respectively, the key elements present in the investigated region are lanthanum (La), phosphate (P), and oxygen (O).[13-14]

DOI : https://doi.org/10.56452/96

3.2 Microstructure

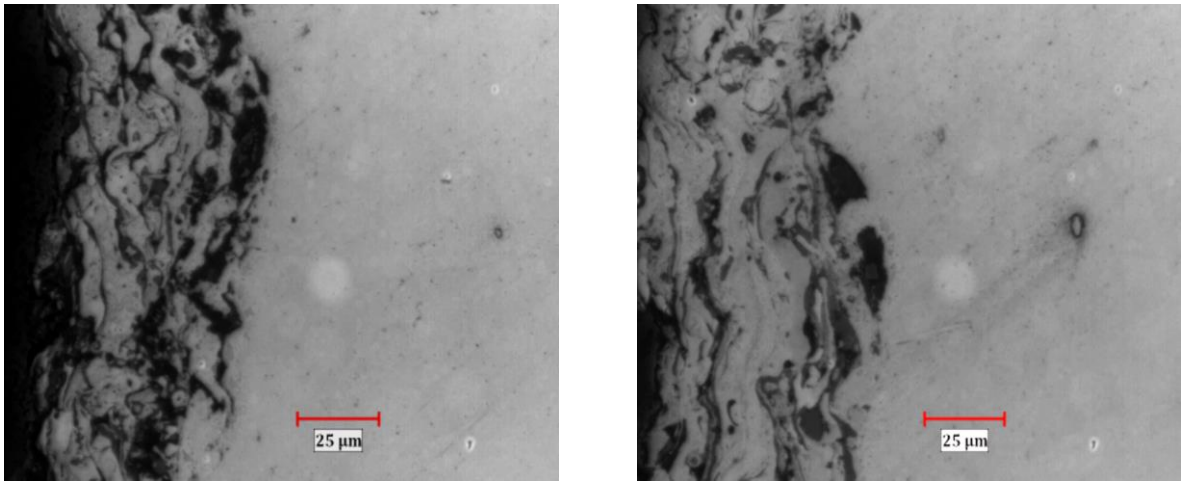

(a) (b)

Figure 4. Optical microstructure of Inconel-625 in cross-sectional view coated with (a) Lanthanum Zirconate; (b) Lanthanum Phosphate.

Figure 4. depicts the coating of lanthanum zirconate and lanthanum phosphate on Inconel-625 substrate in cross-section, showing splats and ensuring that the coated surface is dense and homogeneous. Bond coat included, the developed coating has a thickness of around 150 µm. The microstructure of base material consists of uniform distribution of carbides along the grain boundary of Nickel solid solution.

3.3 X-Ray Diffraction

3.3.1 Inconel 625 coated with Lanthanum Zirconate

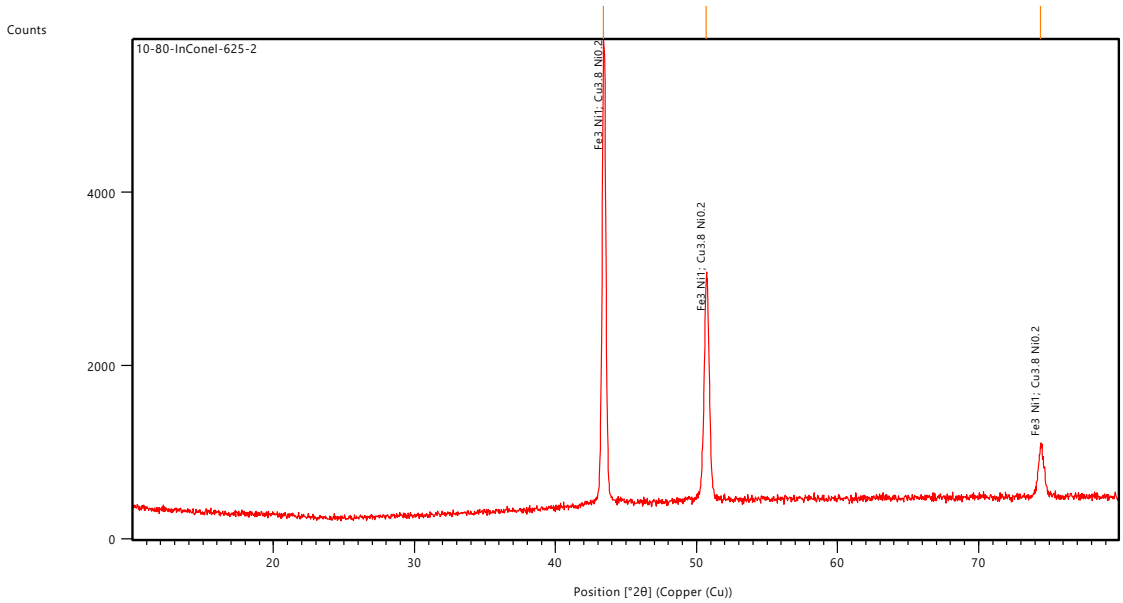

Figure 5. Inconel 625 coated with Lanthanum Zirconate

To determine the phases crystalline that material contains and to learn more about its chemical makeup, XRD analysis is used. The composition of lanthanum zirconate (LZ) and its pattern are shown in the figure 5. LZ

DOI : https://doi.org/10.56452/96

has a cubic phase at room temperature, which has been studied. LZ does not undergo any phase changes between ambient temperature and its melting point. Only one LZ cubic phase is present from ambient temperature until its melting point when the molar ratio of ZrO_2 and La_2O_3 is 2:1, which equates to 33.3 percent La_2O_3. From Figure 5, the reflections were observed for pyrochlore phase at 43.41° (100%), 50.68° (43.77%), 74.38°(11.31%) for Iron Nickel with chemical formula Fe3 Ni1 and Copper Nickel with chemical formula Cu3.8 Ni0.2.

3.3.2 Inconel 625 coated with Lanthanum Phosphate

Figure 6. shows the plasma spray coated samples' X-ray diffraction patterns of lanthanum phosphate particles . From Figure 6. the reflections were observed for pyrochlore phase at 29.98° (8.32%), 35.39° (8.99%), 40.48°(100%), 43.42° (40.08%), 44.129° (37.03%), 48.57°(5.45%), 58.63°(21.94%), 73.70°(33.85%) for Molybdenum Niobium Nickel with chemical formula Mo28 Nb1.12 Ni26.88 and Chromium Nickel Silicide with chemical formula Cr3 Ni2 Si1.

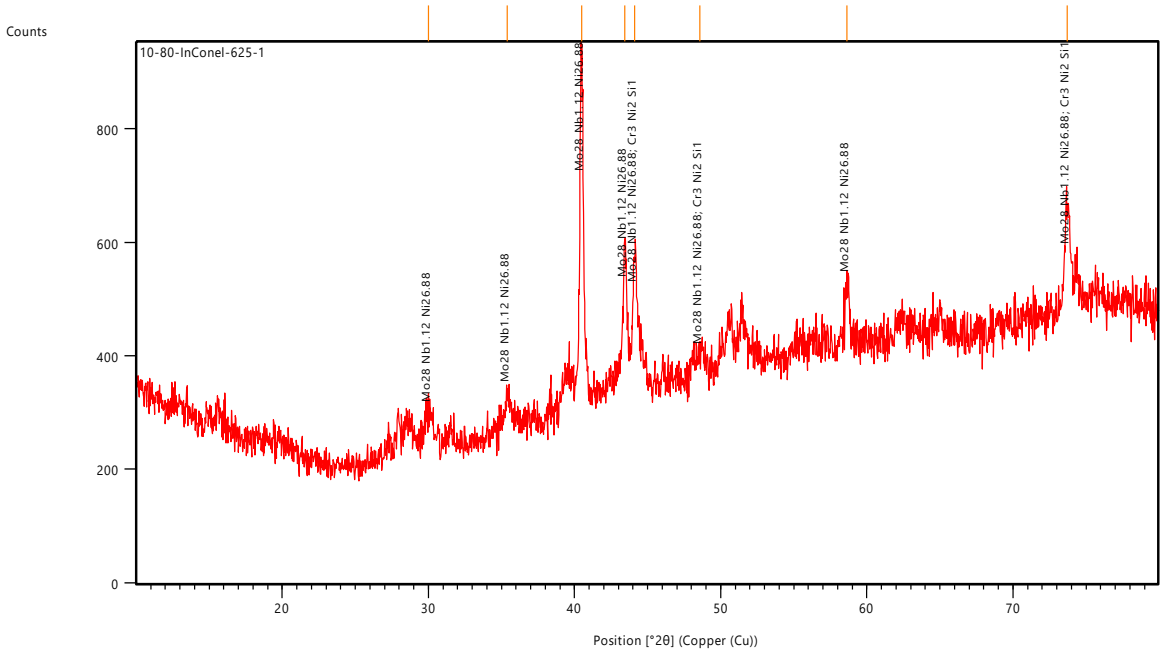

Figure 6. Inconel 625 coated with Lanthanum Phosphate

3.4 Mechanical Properties of Lanthanum Zirconate and Lanthanum Phosphate

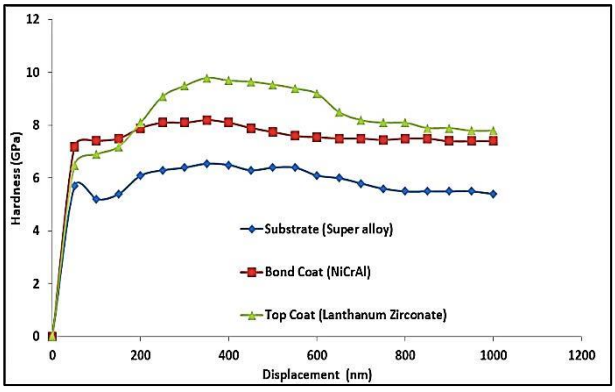

Figure 7. Hardness variations in lanthanum zirconate coatings

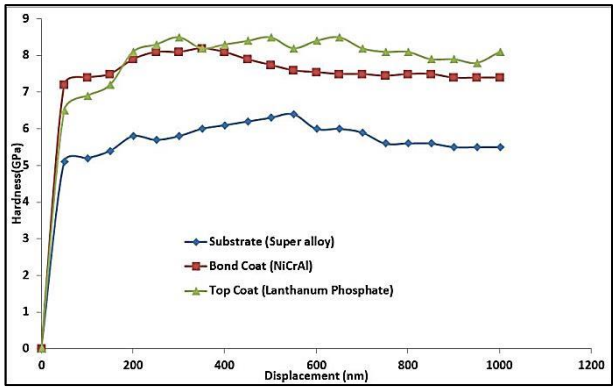

Figure 8. Hardness variations in Lanthanum phosphate coatings

DOI : https://doi.org/10.56452/96

Figure 7. presents variation of the hardness of the lanthanum zirconate coatings with respect to displacement. As expected the lanthanum zirconate coating have exhibited superior hardness compared to bond coat and substrate alloy. The highest hardness of 9.8 GPa is recorded in lanthanum zirconate coatings at a displacement of 400 nm. whereas the bond coat has exhibited hardness value in the range of 7-8 GPa. The substrate hardness varies in the range of 5.5 to 6 GPa. Figure 8. presents the hardness variations in lanthanum phosphate coatings. The hardness value varies between 8-10 GPa in case of topcoat. The bond coat has exhibited a highest hardness 8.2GPa at a displacement of 400nm. Owing to superior mechanical properties lanthanum zirconate coatings have exhibited the highest hardness compared to lanthanum phosphate coatings.

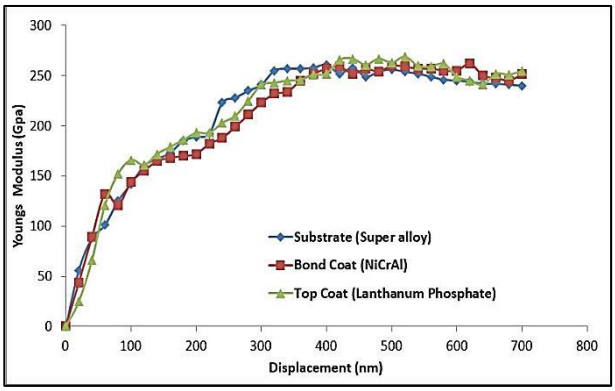

Figure 9. Young's modulus variations in lanthanum phosphate coatings

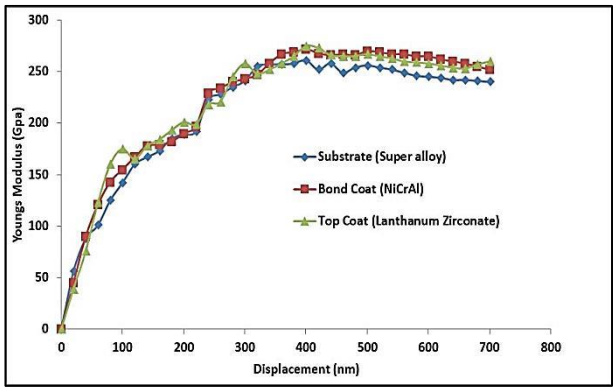

Figure 10 Young's modulus variations in lanthanum zirconate coatings

The young's modulus variations of lanthanum based TBCs with displacement are presented in Figure 9 and Figure 10. Compared to bond coat and substrate alloy, the lanthanum-based coatings have been shown to have better young modulus. Lanthanum zirconate coatings at displacement of 400 nm record the highest young modulus of 280 GPa. In the range from 240 to 260 GPa, the bond coat had a young's module value for with displacement. The young modulus of substrate fluctuates between 230 and 250 GPa. The differences in young's modulus of lanthanum zirconate coatings are seen in Figure 10. The young modulus variations in lanthanum phosphate coatings are described in Figure 9. In the case of a top coat, the young modulus value fluctuates between 270-280 GPa. At a displacement of 400nm, the bond coat showed a maximum modulus of 275 GPa. Lanthanum zirconate coatings have a higher hardness than lanthanum phosphate coatings because of greater mechanical characteristics.

4. Conclusion

1. TBCs based on Lanthanum Zirconate and Lanthanum Phosphate were effectively produced on Inconel-625 super alloy utilizing the Air Plasma Spray (APS) technique in this study. Mechanical properties like Young's modulus and micro hardness behaviour of the coated samples were all measured and compared.
2. Lanthanum Zirconate coatings posses higher hardness compared to Lanthanum phosphate coatings because of superior mechanical properties.
3. Lanthanum zirconate coatings posses higher value of young's modulus compared to lanthanum phosphate coatings because of greater mechanical properties.

5. References

[1]Jing Zhang, Xingye Guo, Yeon-Gil Jung, Li Li, James Knapp, "Lanthanum zirconate based thermal barrier coatings: A review", Surface & Coatings Technology (2016), DOI: 10.1016/j.surfcoat.2016.10.019.

[2]Emine Bakan, Robert Vaben, "Ceramic Top Coats of Plasma-Sprayed Thermal Barrier Coatings: Materials, Processes, and Properties", (2017) 26:992–1010, DOI 10.1007/s11666-017-0597-7.

[3]Georg Mauer, Linnan Du and Robert Vaben, "Atmospheric Plasma Spraying of Single Phase Lanthanum Zirconate Thermal Barrier Coatings with Optimized Porosity", 2016, 6, 49; doi:10.3390/coatings6040049.

[4]A. Pragatheeswaran, P.V. Ananthapadmanabhan, Y. Chakravarthy, Subhankar Bhandari, Vandana Chaturvedi, Nagaraj A, K. Ramachandran, "Plasma spray-deposited lanthanum phosphate coatings for protection against molten uranium corrosion", doi 10.1016/j.surfcoat.2015.01.040.

[5]Xingye Guo, Zhe Lu, Yeon-Gil Jung, Li Li, James Knapp and Jing Zhang, "Thermal Properties, Thermal Shock, and Thermal Cycling Behavior of Lanthanum Zirconate-Based Thermal Barrier Coatings", DOI: 10.1007/s40553-016-0070-4.

[6]Jing Zhang, Xingye Guo, Yi Zhang, Zhe Lu, Hyun-Hee Choi, Yeon-Gil Jung, In-Soo Kim, "Mechanical Properties of Lanthanum Zirconate Based Composite Thermal Barrier Coatings" Advances in Applied Ceramics · January 2019, DOI: 10.1080/17436753.2018.1564415.

[7]Jing Zhang, Xingye Guo, Yi Zhang, Zhe Lu, Hyun-Hee Choi, Yeon-Gil Jung & In-Soo Kim (2019), "Mechanical properties of lanthanum zirconate-based composite thermal barrier coatings", Advances in Applied Ceramics, 118:5, 257-263, DOI: 10.1080/17436753.2018.1564415.

[8]S.K. Mishra, N. Jagdeesh, and L.C. Pathak, "Fabrication of Nanosized Lanthanum Zirconate Powder and Deposition of Thermal Barrier Coating by Plasma Spray Process", JMEPEG (2016) 25:2570–2575, DOI: 10.1007/s11665-016-2122-4.

[9]A. Mehta, H. Vasudev and S. Singh, "Recent developments in the designing of deposition of thermal barrier coatings – A review", Materials Today: Proceedings, https://doi.org/10.1016/j.matpr.2020.02.271.

[10]Sankar Sasidharan, Rajesh Komban, Shijina Nambiar, Balagopal N. Nair, M. Padmanabhan, Krishna G. Warrier and U.S. Hareesh, "Sol-Gel Lanthanum Phosphate: A Versatile Ceramic Material for Diverse Functional Applications", Advances in Sol-Gel Derived Materials and Technologies, DOI 10.1007/978-3-319-50144-4_10.

[11]D. Chellaganesh, M. Adam Khan, J.T. Winowlin Jappes, "Thermal barrier coatings for high temperature applications – A short review", https://doi.org/10.1016/j.matpr.2020.08.017.

[12]Ali Avci, Aysegul A. Eker, Bulent Eker, "Microstructure and Oxidation behavior of atmospheric plasma sprayed Thermal Barrier Coatings", http://dx.doi.org/10.1016/B978-0-12-813734-5.00045-7.

[13]Deepthi T, K. Balamurugan, "Effect of Yttrium (20%) doping on mechanical properties of rare earth nano lanthanum phosphate (LaPO4) synthesized by aqueous sol-gel process", Ceramics International 45 (2019) 18229–18235.

[14]G. Moskal, L. Swadzba, M. Hetmanczyk, B. Witala, B. Mendala, J. Mendala, P.Sosnowy. "Characterisation of the microstructure and thermal properties of Nd2Zr2O7 and Nd2Zr2O7/YSZ thermal barrier coatings", doi:10.1016/j.jeurceramsoc.2011.12.004.